2016 IEEE International Conference on Advanced Intelligent Mechatronics (AIM)
Banff, Alberta, Canada, July 12–15, 2016

A Fully Actuated Quadrotor UAV with a Propeller Tilting Mechanism: Modeling and Control

Marcin Odelga, Paolo Stegagno and Heinrich H. Bülthoff

***Abstract*— Equipped with four actuators, quadrotor Unmanned Aerial Vehicles belong to the family of underactuated systems. The lateral motion of such platforms is strongly coupled with their orientation and consequently it is not possible to track an arbitrary 6D trajectory in space. In this paper, we propose a novel quadrotor design in which the tilt angles of the propellers with respect to the quadrotor body are being simultaneously controlled with two additional actuators by employing the parallelogram principle. Since the velocity of the controlled tilt angles of the propellers does not appear directly in the derived dynamic model, the system cannot be static feedback linearized. Nevertheless, the system is linearizable at a higher differential order, leading to a dynamic feedback linearization controller. Simulations confirm the theoretical findings, highlighting the improved motion capabilities with respect to standard quadrotors.**

I. Introduction

Multirotor Unmanned Aerial Vehicles (UAVs), being not constrained by ground conditions, can operate on places that are out of reach for other classical mobile robots. They offer high maneuverability, vertical take-off and landing, hovering mode, and other features that make it a popular platform for many robotic applications such as inspection, exploration, surveillance, data collection, and recently also aerial manipulation (see [1] and references therein).

One of the limitations of quadrotors (and other multirotors with coplanar propellers) is their intrinsic underactuation. A change in position or disturbance counteraction of such an UAV involves a change in its orientation. Although this may not impose any significant restraint in open-air flights, it might be crucial when the precision of control matters or in presence of external disturbances, e.g., an abrupt or unwanted change in orientation might involve the need of incommodious rectification of directional sensor measurements. For instance, stabilization of the visual feedback from a vehicle is an important factor affecting performance in teleoperation tasks, especially in obstacle rich environments (see for example [2] and [3]). In physical interaction involving either a direct contact [4] or additional robotic arms attached to the multirotor body [5], the lack of controllability over some degrees of freedom (DOFs) can significantly complicate the control task, e.g., by requiring higher order differentiation of the system model, hence measurements of higher order derivatives of the system state.

M. Odelga, P. Stegagno and H. H. Bülthoff are with the Max Planck Institute for Biological Cybernetics, Department of Human Perception Cognition and Action, Spemannstrasse 38, 72076 Tübingen, Germany {modelga, pstegagno, hhb}@tuebingen.mpg.de

M. Odelga is also with the University of Tübingen, Tübingen, Germany

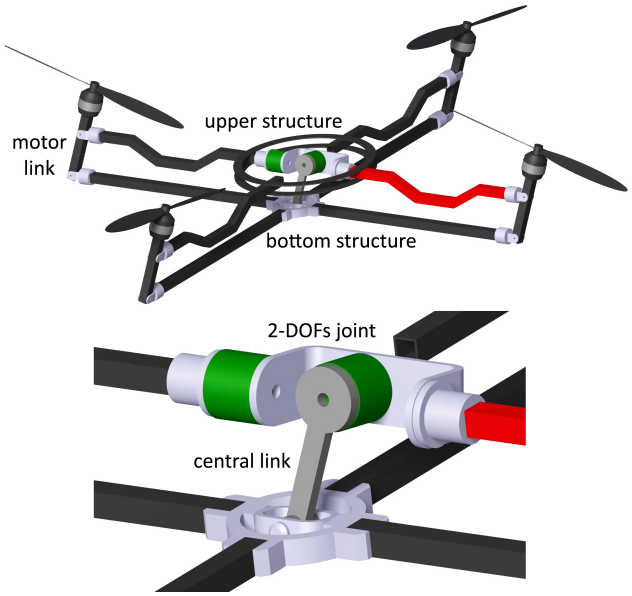

Fig. 1. Top: conceptual CAD model of the proposed platform; bottom: the tilting mechanism in detail; in green, the two additional actuators; in gray, the joints of the platform; the red arm indicates the forward direction.

One of the common solutions, mostly in aerial photography, is the use of additional stabilization devices (e.g., camera gimbals [6]) that decouple the sensor rotation from the orientation of the platform. Another approach, for which we propose a novel concept in this paper, is to expand the controllability by additional actuated DOFs. Different concepts can be found in literature. One common approach is the employment of fixed tilted propellers [7], [8], which however, requires constant counterbalance and energy dissipation of extra forces and torques. For this reason, the values of the tilt angles are usually optimized for certain range of trajectories. Another approach is to add auxiliary propellers [9] or a wing/rotor tilting mechanism [10], [11], [12]. Platforms equipped with additional actuators share some drawbacks, e.g., loss of efficiency from the increased weight, and higher power consumption.

Inspired by the latter research, in this paper we propose a novel platform with two additional actuators that allow to simultaneously change the orientation of all propellers. In Fig. 1, we show a conceptual 3D design of the platform and its kinematic diagram in Fig. 2. The main novelty, and in our opinion the most interesting property of this design, is that it allows to control 6 DOFs with six input, thus it does not require optimization due to redundant control inputs nor suffers it from energy dissipation due to an internal wrench caused by counteracting actuators.

978-1-5090-2065-2/16/$31.00 ©2016 IEEE

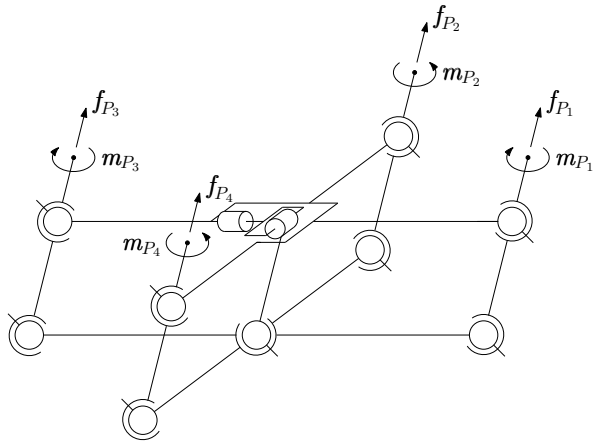

Fig. 2. Kinematic diagram of the platform.

The rest of this paper is organized as follows. In Sec. II we describe the proposed mechanism and we derive the dynamical model of the fully actuated quadrotor. In Sec. III we derive the equations for the dynamic feedback linearization and we propose a controller for the platform. Section IV presents simulation results which highlight the improved motion capabilities with respect to a standard quadrotor and Section V concludes the paper.

II. Platform Description

In order to control a classical quadrotor to perform a motion along a given trajectory, the accumulated thrust of the four propellers must be directed towards the desired direction while simultaneously counteracting the gravity force and other external disturbances [1]. Although the rotation of the platform can be induced with the resulting torque, only the angle around the vertical axis (usually Z) can be controlled independently whilst the other two are used to orient the thrust as stated above.

In order to decouple the lateral motion from the tilt angles of the platform and thus regain the control over the two missing degrees of freedom, we have designed a model with a propeller tilting mechanism that can change the orientation of the produced thrust. This tilting mechanism, depicted in Figs. 1 and 2, is made of a 2-DOFs actuated joint, a central link, and the bottom structure (the four bottom arms in the figures) that transfer the motion to the motor links. The central link, bottom structure, platform's arms and motor links form four parallelograms coupled with the central link allowing the simultaneous tilt of all the propellers.

In the derivation process of the dynamic model of our platform, presented later in this Section, we assume that the motion of the bottom structure is negligible with respect to the dynamics of the UAV. This assumption is motivated by the fact that the broad majority of the system's components (e.g.: battery, computational unit, etc.), hence the mass, can be located around the center of the upper structure. With the design presented in Fig. 1, the tilting angles are limited to the interval $[-\frac{\pi}{6}, \frac{\pi}{6}]$. The effect of this constraint will be further discussed in Section IV.

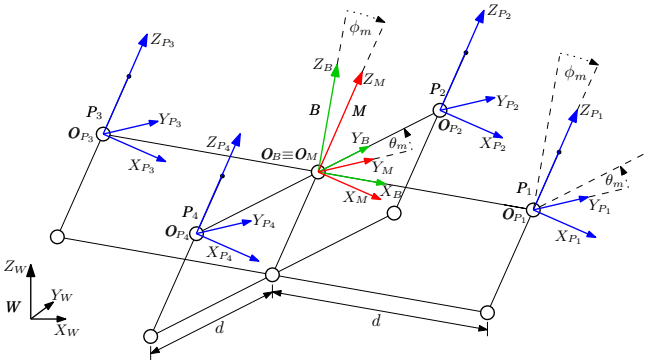

Fig. 3. Simplified diagram of the platform with depicted coordinate frames: $\boldsymbol{W}$ in black, $\boldsymbol{B}$ in green, $\boldsymbol{M}$ in red and $\boldsymbol{P}_i, i = 1, \ldots, 4$ in blue.

A. Notation and Definitions

We represent the relevant quantities in the following reference frames, depicted in Fig. 3: a global inertial frame of reference $\boldsymbol{W} : \{\boldsymbol{O}_W, X_W, Y_W, Z_W\}$; a moving body frame $\boldsymbol{B} : \{\boldsymbol{O}_B, X_B, Y_B, Z_B\}$ attached to the quadrotor at its center of mass, ideally the middle point between the propellers; the tilting mechanism frame $\boldsymbol{M} : \{\boldsymbol{O}_M, X_M, Y_M, Z_M\}$ with $\boldsymbol{O}_M \equiv \boldsymbol{O}_B$; and a set of four frames attached to the centers of propellers $\boldsymbol{P}_i : \{\boldsymbol{O}_{P_i}, X_{P_i}, Y_{P_i}, Z_{P_i}\},\ i = 1 \ldots 4$.

To represent the relative pose of two arbitrary frames, e.g., $\boldsymbol{A}$ in $\boldsymbol{B}$, we will use the classical rotation matrix notation ${}^B\boldsymbol{R}_A \in SO(3)$ for orientation, and consequently, ${}^B\boldsymbol{p}_A = {}^B\boldsymbol{O}_A \in \mathbb{R}^3$ for position. Therefore, we define the platform position and orientation in the global frame $\boldsymbol{W}$ as $\boldsymbol{p} = {}^W\boldsymbol{p}_B = (p_x\ p_y\ p_z)^T$ and

$$\boldsymbol{R}_B = {}^W\boldsymbol{R}_B = \boldsymbol{R}_z({}^W\psi_B)\boldsymbol{R}_y({}^W\theta_B)\boldsymbol{R}_x({}^W\phi_B),$$

respectively, where ${}^W\phi_B = \phi_B$, ${}^W\theta_B = \theta_B$, ${}^W\psi_B = \psi_B$ denote the roll, pitch and yaw rotation angles of the platform, and $\boldsymbol{R}_x(\cdot)$, $\boldsymbol{R}_y(\cdot)$, $\boldsymbol{R}_z(\cdot)$, the canonical rotation matrices representing the elemental rotations around the X, Y and Z axes.

In a classical quadrotor the thrust is directed along the vertical axis Z_B of the body frame. In our design, by reorienting the propellers with the tilting mechanism, the force can be applied independently of the body rotation along the new direction Z_M defined such that

$${}^B\boldsymbol{R}_M = \boldsymbol{R}_y(\theta_m)\boldsymbol{R}_x(\phi_m).$$

where ${}^B\phi_M = \phi_m$ and ${}^B\theta_M = \theta_m$ are the roll and pitch angles of the tilting mechanism. As a result of the coupled four parallelograms that link the tilting mechanism with the motor links, the orientation of each i-th propeller ${}^B\boldsymbol{R}_{P_i}$ is identical and equal to the orientation of the tilting mechanism

$${}^B\boldsymbol{R}_{P_i} = {}^B\boldsymbol{R}_M, \qquad i = 1 \ldots 4,$$

and their positions are defined as

$$\boldsymbol{O}_{P_i} = {}^B\boldsymbol{O}_{P_i} = \boldsymbol{R}_z\left((i-1)\pi/2\right)\begin{bmatrix} d \\ 0 \\ 0 \end{bmatrix}, \qquad i = 1 \ldots 4, \tag{1}$$

with d being the arm length - the distance from the centers of the propellers to the center of mass of the UAV.

$$\boldsymbol{F}_m = \begin{bmatrix} k_f c_{\phi_m} s_{\theta_m} & k_f c_{\phi_m} s_{\theta_m} & k_f c_{\phi_m} s_{\theta_m} & k_f c_{\phi_m} s_{\theta_m} \\ -k_f s_{\phi_m} & -k_f s_{\phi_m} & -k_f s_{\phi_m} & -k_f s_{\phi_m} \\ k_f c_{\phi_m} c_{\theta_m} & k_f c_{\phi_m} c_{\theta_m} & k_f c_{\phi_m} c_{\theta_m} & k_f c_{\phi_m} c_{\theta_m} \end{bmatrix} \tag{8}$$

$$\boldsymbol{\tau}_m = \begin{bmatrix} -k_m c_{\theta_m} s_{\phi_m} & dk_f c_{\theta_m} c_{\phi_m} + k_m c_{\theta_m} s_{\phi_m} & -k_m c_{\theta_m} s_{\phi_m} & -dk_f c_{\theta_m} c_{\phi_m} + k_m c_{\theta_m} s_{\phi_m} \\ -dk_f c_{\phi_m} c_{\theta_m} + k_m s_{\phi_m} & -k_m s_{\phi_m} & dk_f c_{\phi_m} c_{\theta_m} + k_m s_{\phi_m} & -k_m s_{\phi_m} \\ -dk_f s_{\phi_m} - k_m c_{\phi_m} c_{\theta_m} & -dk_f c_{\phi_m} s_{\theta_m} + k_m c_{\phi_m} c_{\theta_m} & dk_f s_{\phi_m} - k_m c_{\phi_m} c_{\theta_m} & dk_f c_{\phi_m} s_{\theta_m} + k_m c_{\phi_m} c_{\theta_m} \end{bmatrix} \tag{9}$$

B. Dynamic Equation of Motion

Exploiting the common Newton-Euler approach, we start with defining the forces and torques acting on the platform. We assume the following simplified model of a propeller:

$$\begin{cases} \boldsymbol{f}_{P_i} = (0\ 0\ k_f \bar{w}_i |\bar{w}_i|)^T, & k_f > 0, \\ \boldsymbol{m}_{P_i} = (0\ 0\ -k_m \bar{w}_i |\bar{w}_i|)^T, & k_m > 0, \end{cases} \tag{2}$$

in which the produced thrust $\boldsymbol{f}_{P_i}$ and the reaction moment $\boldsymbol{m}_{P_i}$ in the propeller frame $\boldsymbol{P}_i, i = 1 \dots 4$ are proportional to the signed square spinning velocity of the rotor $w_i = \bar{w}_i |\bar{w}_i|$, $i = 1 \dots 4$ with factors k_f and $-k_m$, respectively. The factors k_f and k_m are thrust and torque propeller's coefficients, e.g., can be obtained experimentally [10]. Although this approach does not model any first- or second-order aerodynamic effects (e.g., the different thrust between the advancing and retreating blades or blade flapping), as validated in [10], (2) accurately captures the dynamics of a propeller. In addition we assume that the actuators of the tilting mechanism have high gain fast dynamics.

Hence, we can obtain the total propellers thrust ${}^B\boldsymbol{T} \in \mathbb{R}^3$ and torque ${}^B\boldsymbol{\tau} \in \mathbb{R}^3$ acting on the center of mass

$${}^B\boldsymbol{T} = \sum_{i=1}^{4} {}^B\boldsymbol{R}_{P_i} \boldsymbol{f}_{P_i}, \tag{3}$$

$${}^B\boldsymbol{\tau} = \sum_{i=1}^{4} {}^B\boldsymbol{R}_{P_i} \boldsymbol{m}_{P_i} + \sum_{i=1}^{4} \left({}^B\boldsymbol{O}_{P_i} \times {}^B\boldsymbol{R}_{P_i} \boldsymbol{f}_{P_i} \right), \tag{4}$$

Substituting (3) and (4) to the Newton-Euler set of equations

$$\begin{aligned} \boldsymbol{R}_B {}^B\boldsymbol{T} &= m \left(\ddot{\boldsymbol{p}} - \begin{bmatrix} 0 \\ 0 \\ -g \end{bmatrix} \right), \\ {}^B\boldsymbol{\tau} &= \boldsymbol{I}_B \dot{\boldsymbol{\omega}}_B + \boldsymbol{\omega}_B \times \boldsymbol{I}_B \boldsymbol{\omega}_B, \end{aligned} \tag{5}$$

yields the dynamic model of our system:

$$\begin{aligned} \begin{bmatrix} \ddot{\boldsymbol{p}} \\ \dot{\boldsymbol{\omega}}_B \end{bmatrix} &= \begin{bmatrix} \boldsymbol{g} \\ \mathbf{c} \end{bmatrix} + \begin{bmatrix} \frac{1}{m}\boldsymbol{R}_B & \mathbf{0} \\ \mathbf{0} & \boldsymbol{I}_B^{-1} \end{bmatrix} \begin{bmatrix} \frac{\partial {}^B\boldsymbol{T}}{\partial \boldsymbol{w}} & \frac{\partial {}^B\boldsymbol{T}}{\partial \boldsymbol{\omega}_m} \\ \frac{\partial {}^B\boldsymbol{\tau}}{\partial \boldsymbol{w}} & \frac{\partial {}^B\boldsymbol{\tau}}{\partial \boldsymbol{\omega}_m} \end{bmatrix} \begin{bmatrix} \boldsymbol{w} \\ \boldsymbol{\omega}_m \end{bmatrix} \\ &= \begin{bmatrix} \boldsymbol{g} \\ \mathbf{c} \end{bmatrix} + \begin{bmatrix} \frac{1}{m}\boldsymbol{R}_B & \mathbf{0} \\ \mathbf{0} & \boldsymbol{I}_B^{-1} \end{bmatrix} \begin{bmatrix} \boldsymbol{F}_m & \mathbf{0} \\ \boldsymbol{\tau}_m & \mathbf{0} \end{bmatrix} \begin{bmatrix} \boldsymbol{w} \\ \boldsymbol{\omega}_m \end{bmatrix} \\ &= \boldsymbol{f} + \boldsymbol{J}_R \begin{bmatrix} \boldsymbol{J}_m & \mathbf{0} \end{bmatrix} \begin{bmatrix} \boldsymbol{w} \\ \boldsymbol{\omega}_m \end{bmatrix} = \boldsymbol{f} + \boldsymbol{J} \begin{bmatrix} \boldsymbol{w} \\ \boldsymbol{\omega}_m \end{bmatrix}, \end{aligned} \tag{6}$$

where m is the total mass of the platform, $\boldsymbol{I}_B \in \mathbb{R}^{3\times3}$ is the constant, diagonal and positive-definite inertia matrix, $\boldsymbol{\omega}_B = (\omega_{B_x}\ \omega_{B_y}\ \omega_{B_z})^T$ is the angular velocity of the UAV in $\boldsymbol{B}$,

$$\boldsymbol{f} = [\boldsymbol{g}^T\ \boldsymbol{c}^T]^T = [(0\ 0\ -g)^T\ (-\boldsymbol{I}_B^{-1}(\boldsymbol{\omega}_B \times \boldsymbol{I}_B \boldsymbol{\omega}_B))^T]^T \tag{7}$$

expresses the gravity force acting on the system and the Coriolis term, $[\boldsymbol{w}^T\ \boldsymbol{\omega}_m^T]^T = [(w_1\ w_2\ w_3\ w_4)^T\ (\dot{\phi}_m\ \dot{\theta}_m)^T]^T$ is the control input of the system, and $\boldsymbol{F}_m = \frac{\partial {}^B\boldsymbol{T}}{\partial \boldsymbol{w}}$, $\boldsymbol{\tau}_m = \frac{\partial {}^B\boldsymbol{\tau}}{\partial \boldsymbol{w}}$ are given by equations (8) and (9), respectively ($c_\alpha = cos(\alpha)$ and $s_\alpha = sin(\alpha)$ for $\alpha = \phi_m, \theta_m$).

III. Control

The system obtained in II-B is a non-linear dynamic model, as detailed in [13]. It is always possible to statically feedback linearize such a system if the Jacobian matrix

$$\begin{aligned} \boldsymbol{J} &= \begin{bmatrix} \frac{1}{m}\boldsymbol{R}_B & \mathbf{0} \\ \mathbf{0} & \boldsymbol{I}_B^{-1} \end{bmatrix} \begin{bmatrix} \boldsymbol{F}_m & \mathbf{0} \\ \boldsymbol{\tau}_m & \mathbf{0} \end{bmatrix} \\ &= \begin{bmatrix} \frac{1}{m}\boldsymbol{R}_B \boldsymbol{F}_m & \mathbf{0} \\ \boldsymbol{I}_B^{-1}\boldsymbol{\tau}_m & \mathbf{0} \end{bmatrix} \in \mathbb{R}^{6\times6} \end{aligned} \tag{10}$$

is invertible. Because of the two rightmost null columns of $\boldsymbol{J}$, corresponding to the input $\boldsymbol{\omega}_m$, this condition is not satisfied. Thus, we seek to invert the system at a higher differential order. Derivation of (6) with respect to time gives

$$\begin{aligned} \begin{bmatrix} \dddot{\boldsymbol{p}} \\ \ddot{\boldsymbol{\omega}}_B \end{bmatrix} &= \dot{\boldsymbol{f}} + \dot{\boldsymbol{J}}_R \boldsymbol{J}_{\boldsymbol{m}} \boldsymbol{w} + \boldsymbol{J}_R \dot{\boldsymbol{J}}_m \boldsymbol{w} + \boldsymbol{J}_R \boldsymbol{J}_m \dot{\boldsymbol{w}} \\ &= \begin{bmatrix} \frac{1}{m}\dot{\boldsymbol{R}}_B \boldsymbol{F}_m \boldsymbol{w} \\ \dot{\mathbf{c}} \end{bmatrix} + \boldsymbol{J}_R \begin{bmatrix} \frac{\partial \boldsymbol{F}_m}{\partial \phi_m}\boldsymbol{w} & \frac{\partial \boldsymbol{F}_m}{\partial \theta_m}\boldsymbol{w} \\ \frac{\partial \boldsymbol{\tau}_m}{\partial \phi_m}\boldsymbol{w} & \frac{\partial \boldsymbol{\tau}_m}{\partial \theta_m}\boldsymbol{w} \end{bmatrix} + \boldsymbol{J}_R \boldsymbol{J}_m \dot{\boldsymbol{w}} \\ &= \boldsymbol{J}_R \begin{bmatrix} \boldsymbol{F}_m & \frac{\partial \boldsymbol{F}_m}{\partial \phi_m}\boldsymbol{w} & \frac{\partial \boldsymbol{F}_m}{\partial \theta_m}\boldsymbol{w} \\ \boldsymbol{\tau}_m & \frac{\partial \boldsymbol{\tau}_m}{\partial \phi_m}\boldsymbol{w} & \frac{\partial \boldsymbol{\tau}_m}{\partial \theta_m}\boldsymbol{w} \end{bmatrix} \begin{bmatrix} \dot{\boldsymbol{w}} \\ \boldsymbol{\omega}_m \end{bmatrix} + \begin{bmatrix} \frac{1}{m}\dot{\boldsymbol{R}}_B \boldsymbol{F}_m \boldsymbol{w} \\ \dot{\mathbf{c}} \end{bmatrix} \\ &= \boldsymbol{J}^\star \begin{bmatrix} \dot{\boldsymbol{w}} \\ \boldsymbol{\omega}_m \end{bmatrix} + \begin{bmatrix} \frac{1}{m}\dot{\boldsymbol{R}}_B \boldsymbol{F}_m \boldsymbol{w} \\ \dot{\mathbf{c}} \end{bmatrix}, \end{aligned} \tag{11}$$

where $\boldsymbol{J}^\star$ is the extended Jacobian, $\boldsymbol{w}$ becomes an internal state of the system, and $\dot{\boldsymbol{R}}_B = [\boldsymbol{\omega}_B]_\times \boldsymbol{R}_B$, $[\boldsymbol{\omega}_B]_\times \in so(3)$.

The system (11) can be feedback linearized with a reference input $[\dddot{\boldsymbol{p}}_r^T\ \ddot{\boldsymbol{\omega}}_r^T]^T$ by means of the law

$$\begin{bmatrix} \dot{\boldsymbol{w}} \\ \boldsymbol{\omega}_m \end{bmatrix} = \boldsymbol{J}^{\star -1} \left(\begin{bmatrix} \dddot{\boldsymbol{p}}_r \\ \ddot{\boldsymbol{\omega}}_r \end{bmatrix} - \begin{bmatrix} \frac{1}{m}\dot{\boldsymbol{R}}_B \boldsymbol{F}_m \boldsymbol{w} \\ \dot{\mathbf{c}} \end{bmatrix} \right), \tag{12}$$

which has a solution if $\rho_{J^\star} = rank(\boldsymbol{J}^\star) = 6$, e.i.,

$$\begin{aligned} \det(\boldsymbol{J}^\star) = 8d^2 k_f^5 k_m c_{\phi_m}^2 c_{\theta_m} \\ \cdot (w_1 + w_2 + w_3 + w_4)^2 \neq 0 \end{aligned} \tag{13}$$

Condition (13) is satisfied for $\phi_m, \theta_m \neq \pm\frac{\pi}{2}$ and $w_i > 0,\ i = 1 \dots 4$, which is always fulfilled due to the mechanical constrains of the platform ($|\phi_m|, |\theta_m| < \frac{\pi}{6}$) and the assumption that during flight $w_i > 0,\ i = 1 \dots 4$.

In order to validate the derived system we have employed a linear trajectory tracking controllers for position

$$\dddot{\boldsymbol{p}}_r = \dddot{\boldsymbol{p}}_d + \boldsymbol{K}_{p_1}(\ddot{\boldsymbol{p}}_d - \ddot{\boldsymbol{p}}) + \boldsymbol{K}_{p_2}(\dot{\boldsymbol{p}}_d - \dot{\boldsymbol{p}}) + \boldsymbol{K}_{p_3}(\boldsymbol{p}_d - \boldsymbol{p}), \tag{14}$$

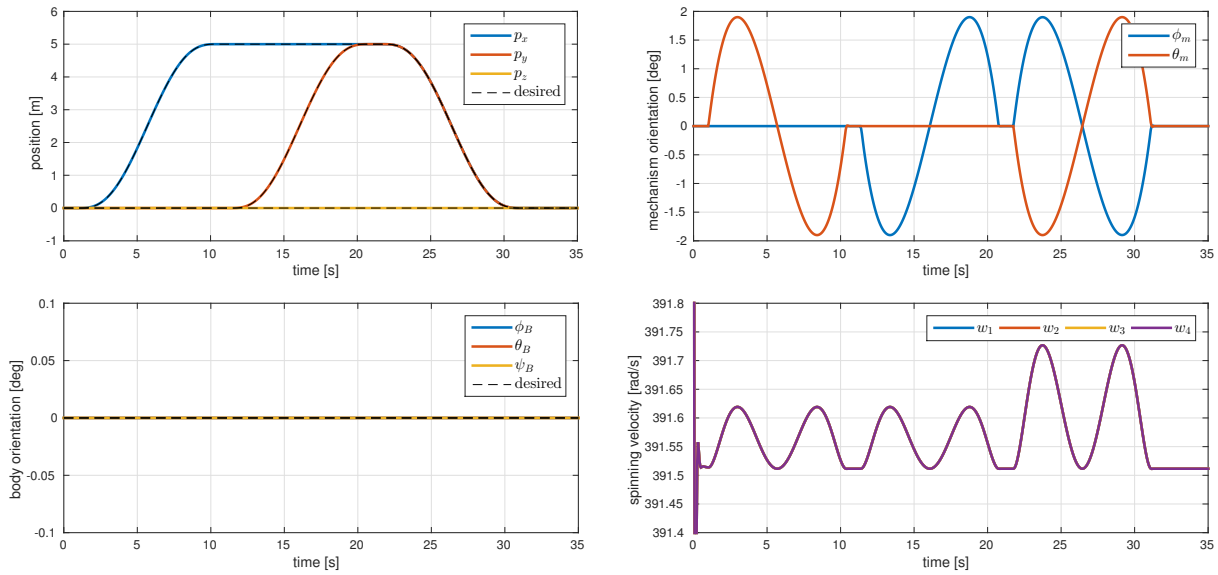

Fig. 4. Results of the first simulation (lateral motion). Top-left: position of the UAV; top-right: orientation of the tilting mechanism; bottom-left: orientation of the UAV; bottom-right: spinning velocities of the propellers.

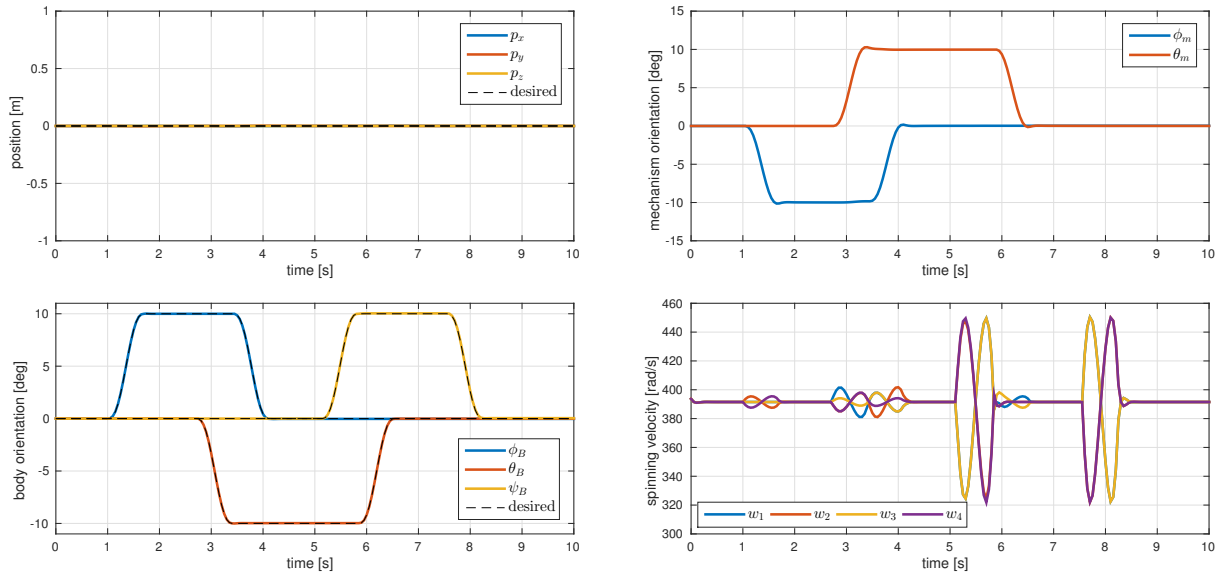

Fig. 5. Results of the second simulation (hovering with non-zero orientation). Top-left: position of the UAV; top-right: orientation of the tilting mechanism; bottom-left: orientation of the UAV; bottom-right: spinning velocities of the propellers.

and orientation

$$\ddot{\boldsymbol{\omega}}_r = \ddot{\boldsymbol{\omega}}_d + \boldsymbol{K}_{\omega_1}(\dot{\boldsymbol{\omega}}_d - \dot{\boldsymbol{\omega}}_B) + \boldsymbol{K}_{\omega_2}(\boldsymbol{\omega}_d - \boldsymbol{\omega}_B) + \boldsymbol{K}_{\omega_3}\boldsymbol{e}_R, \quad (15)$$

as a common approach for feedback linearized systems. The orientation error $\boldsymbol{e}_R$ is defined as

$$\boldsymbol{e}_R = \frac{1}{2}\left[\boldsymbol{R}_B^T\boldsymbol{R}_d - \boldsymbol{R}_d^T\boldsymbol{R}_B\right]_\vee, \quad (16)$$

with $[\cdot]_\vee$ being the inverse map from $so(3)$ to $\mathbb{R}^3$.

Controllers in (14) and (15) ensure [13] an exponential convergence of the tracking error to $\mathbf{0}$ if the gain matrices $\boldsymbol{K}_{p_1}$, $\boldsymbol{K}_{p_2}$, $\boldsymbol{K}_{p_3}$, $\boldsymbol{K}_{\omega_1}$, $\boldsymbol{K}_{\omega_2}$, $\boldsymbol{K}_{\omega_3}$ assure a proper pole placement. The control problem is now defined as an output tracking problem given the desired trajectory in position $\boldsymbol{p}_d$, orientation $\boldsymbol{R}_d$, and their derivatives. It is therefore advisable that the desired trajectories are continuous and derivable up to the 3rd order.

It is necessary, however, to estimate the platform position $\boldsymbol{p}$ and orientation $\boldsymbol{R}_B$, linear and angular velocities, $\dot{\boldsymbol{p}}$ and $\boldsymbol{\omega}_B$, and linear and angular accelerations, $\ddot{\boldsymbol{p}}$ and $\dot{\boldsymbol{\omega}}_B$. Because of the differentiation needed for the dynamic feedback linearization of the model, the actual control inputs $\boldsymbol{w}$, must be numerically integrated from the output of system (12), e.i, $\dot{\boldsymbol{w}}$.

The closed loop system is similar to the one in [10] but due to the one-to-one correspondence between the number of inputs and outputs it is not redundant, thus it does not require optimization.

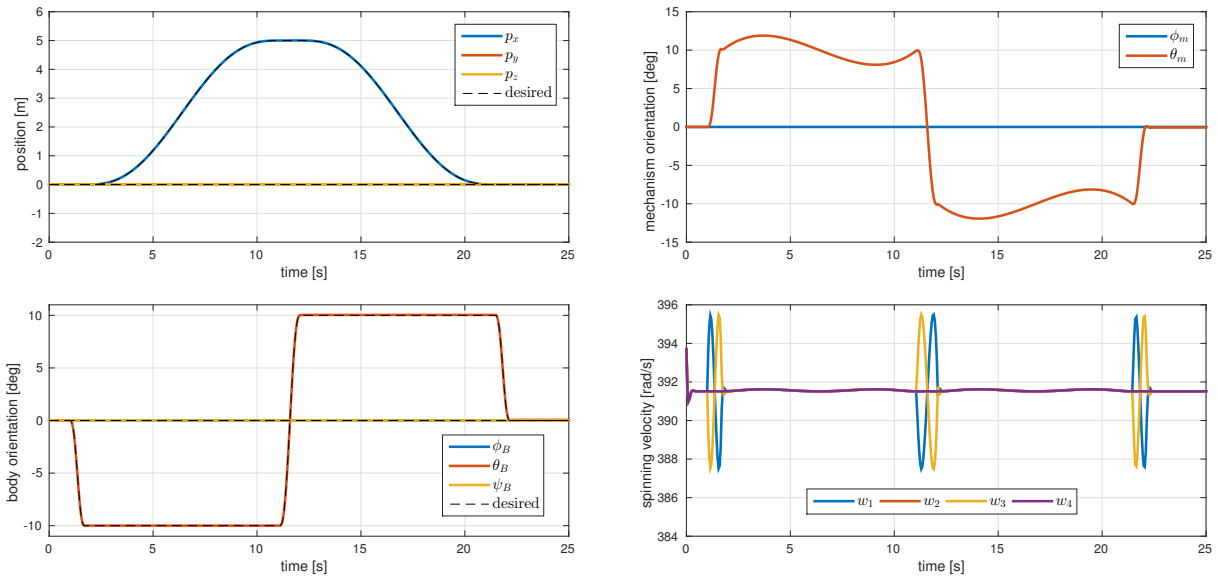

Fig. 6. Results of the third simulation (complex motion). Top-left: position of the UAV; top-right: orientation of the tilting mechanism; bottom-left: orientation of the UAV; bottom-right: spinning velocities of the propellers.

IV. Simulations

In order to validate the model and controller, we have performed numerical simulations of the system in closed loop. In particular, we have tested the ability to perform motions that are not feasible with a normal quadrotor, such as pure translational lateral motion and hovering with non-zero roll and pitch angles.

The trajectory controller designed in Sec. III requires a trajectory defined in position and its derivatives up to the third order (snap). Therefore, the reference trajectories are computed using a fifth-order spline interpolation which generates a smooth trajectory based on the 6D starting and ending point.

For all of the presented simulations we used the following values of the platform parameters: $m = 1\,kg$,

$$\boldsymbol{I}_B = \begin{bmatrix} 0.015\,kg \cdot m^2 & 0 & 0 \\ 0 & 0.015\,kg \cdot m^2 & 0 \\ 0 & 0 & 0.025\,kg \cdot m^2 \end{bmatrix},$$

$k_f = 1.6 \cdot 10^{-5}$, $k_m = 2.5 \cdot 10^{-7}$, $d = 0.3\,m$. The gains of the linear feedback controllers, (14) and (15), were obtained experimentally and set to $\boldsymbol{K}_{p_1} = \boldsymbol{K}_{\omega_1} = 30\boldsymbol{I}_3$, $\boldsymbol{K}_{p_2} = \boldsymbol{K}_{\omega_2} = 600\boldsymbol{I}_3$, and $\boldsymbol{K}_{p_3} = \boldsymbol{K}_{\omega_3} = 900\boldsymbol{I}_3$, where $\boldsymbol{I}_3$ is the 3×3 identity matrix.

Here, we have selected three simulations in which the UAV performs maneuvers which are not feasible with a classical quadrotor.

1) Lateral motion: Figure 4 shows the simulation of a lateral motion with null orientation of the UAV. The desired trajectory is defined as three points such that the platform moves first $5\,m$ along the X_W direction, then $5\,m$ along the Y_W direction, and lastly go back to the initial position $\boldsymbol{p}_0 = (0\ 0\ 0)^T\ m$ while maintaining the orientation ϕ_B, θ_B, $\psi_B = 0°$. As expected, the roll and pitch angles of the mechanism, ϕ_m and θ_m respectively, behave as if they were the roll and pitch angles of a classical quadrotor, thus the body orientation can remain constant. The fluctuation of the spinning velocities w_i, $\in 1 \dots 4$, compensates the additional effects imposed by the movement of the tilting mechanism.

2) Hovering with non-zero orientation: In the second simulation, whose results are shown in Fig. 5, the platform is set to hover in place ($\boldsymbol{p}_d = (0\ 0\ 0)^T$) while the UAV orientation angles, ϕ_B, θ_B and ψ_B, are controlled. The angles, initially at ϕ_B, θ_B, $\psi_B = 0°$ are in turn brought first to $10°$ and then back to $0°$. The change of roll and pitch of the UAV results in a symmetric behavior of the tilting mechanism in order to compensate them. Instead, by analogy with the classical system, the yaw angle ψ_B can be controlled independently through the input $\boldsymbol{w}$.

3) Complex motion: In the third simulation, Fig. 6, we present a point to point trajectory in which both the position and orientation of the platform, are being changed. It shows that the pitch angle of the body θ_B can be set to a negative value during forward motion (and vice versa) which is not possible for a standard quadrotor.

Remark: The tilt angles of the mechanism, ϕ_m and θ_m, depend on the desired lateral acceleration, as seen in simulation 1), and UAV orientation, ϕ_B and θ_B, simulation 2). Hence, their limit due to the mechanical constraints limits also the feasible motion. For example, it is not possible to hover with any $\phi_B > \max(\phi_m) = \frac{\pi}{6}$. A more rigorous discussion is left for future works.

V. Conclusions

One of the main drawbacks of quadrotors is their underactuation, which causes two rotational degrees of freedom to be strongly coupled with the translational degrees of freedom. In this paper, we have presented a novel design of a fully actuated quadrotor with tilting propellers. After deriving the dynamical model of the platform, we have shown that it

can be feedback linearized in order to design an appropriate control law. Simulations highlight the 6 DOFs capabilities of the platform.

Currently, we are in the process of validating our model and controller with a physical simulator to finalize the design. When the design is finalized, we plan to build the platform and test its capabilities. From the theoretical point of view, we want to study the set of feasible configurations in terms of dynamic velocity and acceleration limits that can be taken into account in the trajectory planning phase.

REFERENCES

[1] R. Mahony, V. Kumar, and P. Corke, "Multirotor aerial vehicles: modeling, estimation, and control of quadrotor," in *IEEE Robotics & Automation Magazine*, vol. 19, no. 3, pp. 20-32, Sept. 2012.

[2] P. Stegagno, M. Basile, H. H. Bülthoff, and A. Franchi, "A semi-autonomous UAV platform for indoor remote operation with visual and haptic feedback," in *2014 IEEE International Conference on Robotics and Automation (ICRA)*, Hong Kong, June 2014, pp. 3862-3869.

[3] M. Odelga, P. Stegagno, and H. H. Bülthoff, "Obstacle detection, tracking and avoidance for a teleoperated UAV," in *2016 IEEE International Conference on Robotics and Automation (ICRA)*, Stockholm, May 2016.

[4] G. Gioioso, M. Ryll, D. Prattichizzo, H. H. Bülthoff and A. Franchi, "Turning a near-hovering controlled quadrotor into a 3D force effector," in *2014 IEEE International Conference on Robotics and Automation (ICRA)*, Hong Kong, June 2014, pp. 6278-6284.

[5] B. Yüksel, S. Mahboubi, C. Secchi, H. H. Bülthoff, and A. Franchi, "Design, identification and experimental testing of a light-weight flexible-joint arm for aerial physical interaction," in *2015 IEEE International Conference on Robotics and Automation (ICRA)* Seattle, WA, 2015, pp. 870-876.

[6] J. M. Hilkert, "Inertially stabilized platform technology, concepts and principles," in *IEEE Control Systems*, vol. 28, no. 1, pp. 26-46, Feb. 2008.

[7] S. Rajappa, M. Ryll, H. H. Bülthoff, and A. Franchi, "Modeling, control and design optimization for a fully-actuated hexarotor aerial vehicle with tilted propellers," in *2015 IEEE International Conference on Robotics and Automation (ICRA)*, Seattle, WA, 2015, pp. 4006-4013.

[8] D. Brescianini, and Raffaello D'Andrea, "Design, modeling and control of an omni-directional aerial vehicle," in *2016 IEEE International Conference on Robotics and Automation (ICRA)*, Stockholm, May 2016.

[9] R. Naldi, L. Gentili, L. Marconi, and A. Sala, "Design and experimental validation of a nonlinear control law for a ducted-fan miniature aerial vehicle," in *Control Engineering Practice*, vol. 18, no. 7, pp. 747-760, July 2010.

[10] M. Ryll, H. H. Bülthoff, and P. R. Giordano, "A Novel Overactuated Quadrotor Unmanned Aerial Vehicle: Modeling, Control, and Experimental Validation," in *IEEE Transactions on Control Systems Technology*, vol. 23, no. 2, pp. 540-556, March 2015.

[11] K. T. Oner, E. Cetinsoy, M. Unel, M. F. Aksit, I. Kandemir, and K. Gulez, "Dynamic model and control of a new quadrotor unmanned aerial vehicle with tilt-wing mechanism," in *Int. Journ. of Mechanical, Aerospace, Industrial and Mechatronics Engineering*, vol. 2, no. 9, pp. 12–17, 2008.

[12] F. Kendoul, I. Fantoni and R. Lozano, "Modeling and control of a small autonomous aircraft having two tilting rotors," in *IEEE Transactions on Robotics*, vol. 22, no. 6, pp. 1297-1302, Dec. 2006.

[13] A. Isidori, *Nonlinear Control Systems*, 3rd ed., Springer-Verlag: Berlin 1995.